Observation of multiple scattering of kHz vibrations in a concrete structure and application to monitoring weak changes

Eric Larose,[1,*] Julien de Rosny,[2] Ludovic Margerin,[1] Domitille Anache,[3] Pierre Gouedard,[1] Michel Campillo,[1] and Bart van Tiggelen[3]

[1]*Laboratoire de Géophysique Interne et Tectonophysique (LGIT), Université J. Fourier and CNRS UMR 5559, Grenoble, France*

[2]*Laboratoire Ondes et Acoustiques (LOA), Université D. Diderot and CNRS UMR 7587, ESPCI, Paris, France*

[3]*Laboratoire de Physique et Modélisation des Milieux Condensés (LPM^{2}C), Université J. Fourier and CNRS, Maison des Magistères, BP 166, 38042 Grenoble, France*

(Received 17 October 2005; published 17 January 2006)

In this paper, we present two experimental studies of mechanical wave propagation in a concrete building around 1 kHz. The first experiment is devoted to the observation of the coherent backscattering enhancement, which demonstrates the presence of multiple diffractions in the late part of the wave records. An application of multiple diffraction and reverberations is proposed in a second experiment. Thanks to their sensitivity to weak changes of the medium, the late records are used to monitor weak change in concrete wave velocity induced by thermal variations. The velocity change measurements have a precision of $\delta c/c = 10^{-4}$. Such a precision is difficult to obtain with direct waves. This experiment is the first step to other applications like stress, damage, aging, or crack monitoring in concrete structures.

DOI: 10.1103/PhysRevE.73.016609 PACS number(s): 43.20.Gp, 43.58.+z, 43.40.+s

I. INTRODUCTION

The dynamic response of concrete structures provides useful information about their mechanical and acoustical properties and has thus been widely studied. For instance, from the main resonant frequencies, one can infer the concrete slab thickness and crack depth [1]. From the attenuation of direct waves, one can also deduce the surface damage [2,3]. Because it is much more complicated to interpret, the late part of the records has always been less studied. This part is made of waves that have traveled very long paths, much longer than the source-sensor distance. These waves have undergone scattering [4,5], absorption, reverberations, diffractions, and interferences before being recorded. They constitute an example of seismic "coda," though at much higher frequencies. One central point in interpreting these late arrivals is to know whether or not they have been simply or multiply scattered or reverberated and diffracted. This is of primary importance for practical applications in imaging or nondestructive testing. Extracting information from diffuse waves is a challenging goal. A great variety of applications of diffuse waves has been proposed in the last 20 years, in optics [6–9], acoustics [10–14], and even more recently in seismology [15–17]. Is the physics developed there applicable to elastic waves in concrete at kHz frequencies?

In a steel reinforced concrete structure of complex shape, we can distinguish two kinds of scattering. The first one is due to the complex geometry which results in random and partial reflections at the lateral sides, edges, and angles. These reverberations and diffractions are present as long as the absorption time is greater than several travel times within the structure, which can be valid for frequencies ranging from Hz to kHz. At low enough frequency (kHz), the complex reverberations due to the structure shape is dominating the coda records. Another scattering phenomena is due to concrete heterogeneities or granularity. This scattering behavior should dominate as soon as the wavelength is of the order of (or smaller than) the size of the heterogeneities or of the steel structure. This was recently observed, for instance by Turner and co-workers [4,5], who have established the diffuse nature of elastic waves in concrete at ultrasonic frequencies.

The purpose of the present paper is first to demonstrate the presence of multiply scattered or multiply reverberated waves in the dynamic response of a concrete structure. This will be done by observing the coherent backscattering enhancement (CBE). Though the physics is not new, CBE has never been observed at kHz frequency for elastic waves in concrete. The second purpose is to propose an application of multiple scattering and/or diffraction of elastic waves. In general, thermal variations of wave velocity in concrete are neglected under ambient conditions (0–40 °C). We will demonstrate the possibility of using the late arrivals (coda waves) to measure velocity changes accurately and then to monitor the temperature.

II. OBSERVATION OF COHERENT BACKSCATTERING

A. Physical principle

CBE is a consequence of interferences in multiple scattering or multiple reverberations of waves in a complex environment. It was first observed for electrons [18] and then in optics [6,7], where it emerged as a doubling of the backscattered energy in the incident direction. Later, it was applied to various field of wave physics, like ultrasounds [11,19], cold atoms [20], and more recently to seismology [16]. In all

*Corresponding author. Present address: Department of Theoretical and Applied Mechanics, University of Illinois, Urbana, Illinois 61801. Email: eric.larose@ujf-grenoble.fr

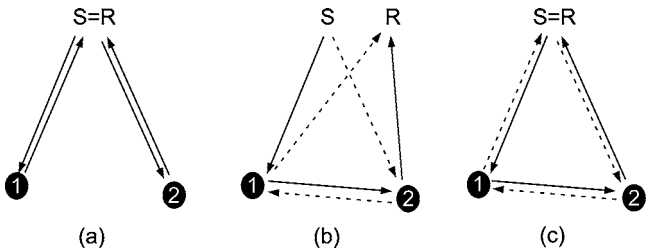

FIG. 1. Example of wave paths. (a) Random interference in the simple scattering regime resulting in a uniform distribution of energy along the array. (b) Random interference of reciprocal paths in the multiple reflection regime with receiver away from the source: uniform energy distribution. (c) Coherent interferences of reciprocal paths in the multiple reflection regime at the source: energy enhancement.

these fields, CBE was shown to be an accurate way to measure transport mean-free paths of the medium, a quantity that characterizes its degree of heterogeneity. CBE finds its origin in the constructive interference between long reciprocal paths in wave scattering or reverberation. This enhances the probability for the wave to return to the source by a factor of exactly 2, which results in the local energy density enhancement by the same factor. For a complete description of WL and CBE, we refer to the review of van Tiggelen and Maynard [21]. In the near field, or if sources and receivers are surrounded by random reflectors, the enhancement width is the order of the wavelength. An heuristic interpretation of this enhancement is given in Fig. 1.

B. Experimental setup and data processing

To observe CBE, we designed an experiment using a linear array of 15 accelerometers. The experimental setup is comparable to the one used by Larose *et al.* [16], except that frequencies are higher by a factor of 100. These accelerometers (Bruel&Kjaer BK-4381) have a nearly flat response in the 10 Hz–5 kHz frequency range (resonant frequency: 16 kHz). To obtain a perfect mechanical coupling, they are glued on the concrete horizontal slab (Fig. 2) using phenylsalicylate. The building is made of several horizontal and vertical, steel-reinforced concrete slabs of width 20 cm. Note that the slabs are mechanically coupled to each other, and that the overall structure has a complex geometry. The main horizontal slab has dimension $12\times5.5\times0.2$ m (see Fig. 2). A hammer strike on the concrete generates the wave. As the impact area is small (1 cm^2) compared to the wavelength, the transient source can be considered as pointlike. Signals are conditioned and acquired immediately using a 24-channel 24-bit acquisition device (Geometrics Stratavisor). The strike triggers the acquisition sequence.

During the CBE experiment, a series of 50 reproducible hammer strikes was performed 5 cm away from receiver i. The 50 records at receiver j are then averaged out, yielding to the impulse response $h_{ij}(t)$ between i and j with a good SNR. The averaging is repeated for each receiver. Moreover this acquisition sequence is repeated for the 15 possible locations of the source. Finally a set of a matrix of 15×15 time-dependent impulse responses is obtained. Each impulse

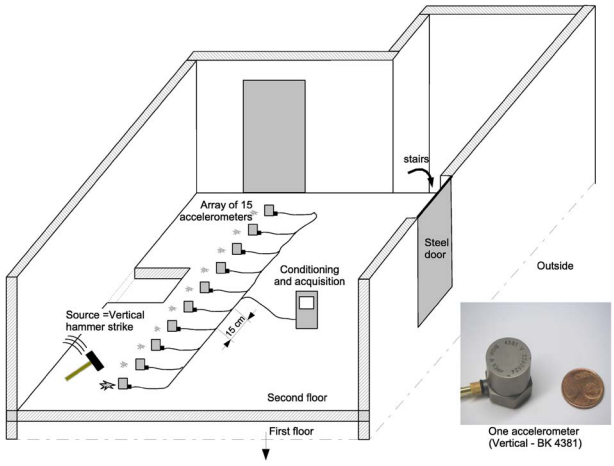

FIG. 2. (Color online) Coherent backscattering effect setup. Fifteen vertical accelerometers (BK-4381) are aligned and stuck on a 20 cm thick concrete slab. The interelement spacing is 15 cm. Each sensor is connected to a conditioning device (Nexus) and then to a 24-bit acquisition device (sampling rate: 16 kHz). The source is a vertical hammer strike 5 cm from the receivers array and is repeated 50 times for each location. The source is also repeated for the 15 different available locations. The concrete structure is a conventional two-level garage, the experiment being conducted on the second floor. Note that not the whole structure is displayed, it is built with several coupled concrete slabs and has a very complex geometry.

response is filtered in the 500–1500 Hz frequency range. At those frequencies, the seismic records last 500 ms before being dominated by the ambient elastic noise. The late arrivals constitute the so-called seismic coda and correspond to travel paths of several hundreds of meters, which is much greater than the concrete structure's characteristic size. Typical wave forms are shown in Fig. 3. The power spectrum is relatively flat in the whole 500–1500 Hz frequency band and is not showing any isolated resonant peak.

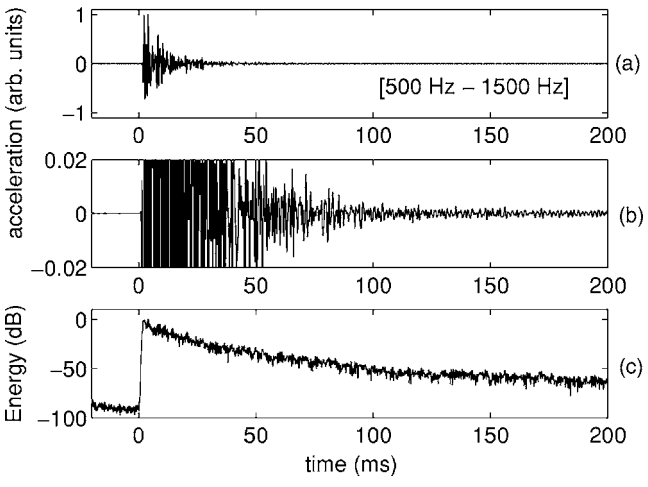

FIG. 3. (a) Example of one acceleration record $h(t)$ near the source. (b) Zoom into the coda. (c) Energy decay of the seismic record. Data are averaged over 50 strikes to reduce the noise level and filtered in the 500–1500 Hz frequency band. The coda is lasting more than 500 ms before reaching the initial noise level.

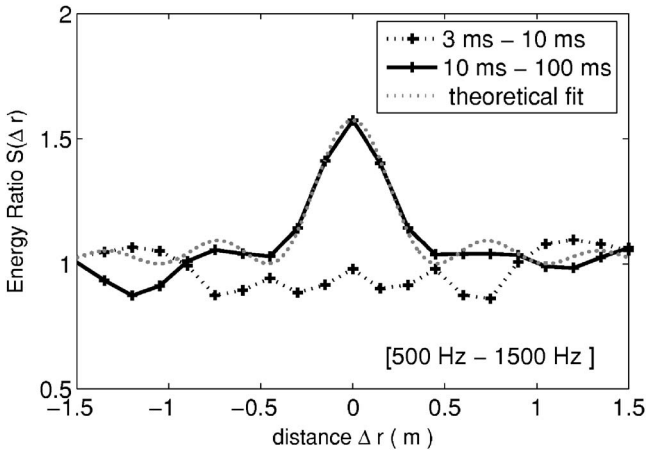

FIG. 4. Energy ratio $S(\Delta r)$ along the receiver array for two consecutive time windows: the early coda (3–10 ms: dotted line with crosses) and the late coda (10–100 ms: continuous line with crosses). The CBE effect corresponds to the energy enhancement around the source ($r=0$) and is observed beyond $t=10$ ms, which provides an estimate of the time between two successive diffractions: $t^* \sim 10$ ms. A theoretical fit is proposed in the gray dotted line. The width of the enhancement cone is the order of the wavelength.

The energy of each impulse response is calculated for different lapse times t,

$$I_{ij} = \int_{t-\delta\tau/2}^{t+\delta\tau/2} h_{ij}^2(\tau) d\tau, \tag{1}$$

where $\delta\tau=1$ ms is the width of the integration window (one cycle of 1 kHz central frequency). In order to extract the CBE enhancement the energy on the jth receiver $[I_{i=i_0;1<j<15}(t)]$ due to the i_0 source is normalized by the averaged energy over different receivers far from the source, corresponding to a distance $|i-j|$ greater than the dominant wavelength λ. This is done to compensate for the coda decay. Thus,

$$S_{ij}(t) = \frac{I_{ij}(t)}{\langle I_{ij}(t)\rangle_{|i-j|>\lambda}}. \tag{2}$$

As for optical or ultrasonic diffuse waves, at a given time and for a given medium, the backscattered intensity shows random fluctuations without any peak around the source. These fluctations are named speckle. This coherent backscattering enhancement is only obtained after averaging out these speckle fluctuations. The first one is achieved over lapse time t. The second is carried out over all the available source-receiver pairs for a given distance Δr between accelerometers i and j. These averagings are assumed to be equivalent to *ensemble averaging*,

$$S(\Delta r) = \langle\langle S_{ij}(t)\rangle_{t\in[T_1;T_2]}\rangle_{|i-j|=\Delta r}. \tag{3}$$

The average energy distribution $S(\Delta r)$ is displayed on Fig. 4 for two different averaging time windows [T1; T2]: the early coda made of direct and simply reflected waves [3 ms;10 ms] and for the late coda [10 ms;100 ms]. The

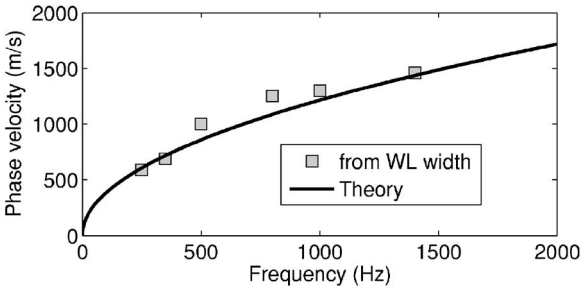

FIG. 5. Theoretical dispersion curve of the A_0 Lamb mode of the slab (solid line). Velocities marked with squares are calculated from the CBE experimental width.

energy enhancement observed for the second time window demonstrates the presence of multiply scattered or multiply reverberated waves and sets approximately the typical time between two successive scattering in the structure around $t^* \approx 10$ ms [16,22,23]. This roughly corresponds to two lateral travel times in the concrete slab, suggesting the coda waves to be due to multiple diffractions in the structure. Hence, the scattering on the concrete internal heterogeneities seems negligible. This is consistent with a central wavelength($\lambda \sim 1$ m) that is much larger than the biggest heterogeneity ($\sim$3 cm) estimated to be present in concrete.

At the working frequencies, the smallest wavelength is still much larger than the slab thickness h. In that case, the vertical-vertical impulse response is dominated by flexural waves (A_0 Lamb waves). Thus, the theoretical distribution for the backscattered intensity in two dimensions for a given wavelength λ is then described by [22]

$$S(\Delta r) = 1 + J_0^2\left(\frac{2\pi}{\lambda} r\right), \tag{4}$$

where J_0 is the Bessel function. A theoretical fit is shown in Fig. 4 (dotted line). We observe that Eq. (4) is in good agreement with the experimental data.

To verify the dependence of the "cone" on the Lamb wavelength, the data were rededuced using six consecutive frequency 0.2 kHz wide band filters. At each frequency, we process the parameter λ of Eq. (4) that best fits the data. The corresponding phase velocity λf is displayed in Fig. 5 (squares). In the same figure, we display the theoretical phase velocity c_φ of the flexural waves (solid line) given by [24]

$$c_\varphi = \sqrt{\frac{2\pi}{\sqrt{3}} fhc_S \sqrt{1 - \frac{c_S^2}{c_P^2}}}. \tag{5}$$

This theoretical curve requires us to know the compressional (c_P) and shear (c_S) wave velocities in bulk concrete. They have been carefully estimated using the experimental configuration depicted in Fig. 6. Two receivers are stuck on the edge of a concrete slab. The P velocity of compression is obtained when the two receivers and the hammer strike (around 1 kHz, 100% BW) are oriented in the direction of propagation (X). We found $c_P=4290$ m/s$\pm$2%. The S velocity ($c_S=2500$ m/s$\pm$2%) was estimated using receivers and

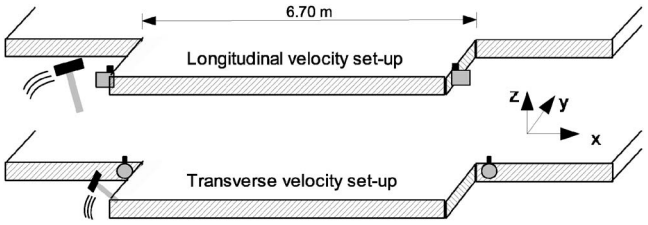

FIG. 6. Sketch of the velocity measurement. Top: Receivers and hammer strikes oriented in the propagation direction to measure the longitudinal velocity. Bottom: Receivers and strikes oriented perpendicularly to the propagation direction to measure the transverse velocity.

hammer strikes perpendicularly oriented to the wave propagation direction (Y). Though these records are dominated by flexural waves, weak first arrivals corresponding to bulk propagation are still visible.

It can be noticed from Fig. 4 that the observed CBE enhancement factor is ~ 1.6. Why not 2 as theoretically expected? Several arguments can be invoked. First, the central receiver is never perfectly at the source, but 5 cm away. Second, the source is never a perfectly vertical hammer strike: its average orientation depends on the operator. These two arguments lower the theoretical enhancement factor 2. Third, the ensemble averaging is not perfect and some speckle fluctuations remain.

As a preliminary conclusion, the CBE effect has been experimentally demonstrated in a complex concrete structure around 1 kHz. This demonstrates the presence of multiple diffraction and reverberations (and possibly some multiple bulk scattering) of seismic waves and provides an elegant way to estimate the scattering mean-free time in the structure. This also confirms previous studies that late arrivals constituting the coda have a deterministic nature, despite the randomness of the wave paths and the unpredictability of the coda wave forms. This opens up new applications for elastic waves in concrete and structure that derive from the physics of multiply scattered or reverberated waves. One of them is the coda wave interferometry.

III. APPLICATION OF CODA WAVE INTERFEROMETRY TO MONITOR WEAK CHANGE OF VELOCITY

A. Physical principle of coda wave interferometry

The idea of the present section is to take advantage of multiply scattered and/or reflected waves. They have traveled much longer paths than direct waves and are, therefore, much more sensitive to weak variations of the medium. The possibility of monitoring weak changes with seismic coda waves is not new. One of the first attempts was reported by Poupinet *et al.* [25] in 1984. They used seismic doublets in a volcano to monitor its internal geological change. In the late 80s, an analogous principle, called diffuse wave spectroscopy (DWS), was developed in optics and applied to quantify the Brownian motion of particle suspension using light scattering [8]. A similar application was developed in acoustics, diffuse acoustical wave scattering (DAWS) [26,27]. More recently, DAWS was applied to ultrasonic reverberant cavities [28,29], diffuse reverberant acoustical wave scattering (DRAWS) to quantify the scattering strength and the motion statistics of random scatterers (e.g., a school of fish in a water tank).

Applications were also developed in reverberant or open systems to a global change of the medium property: the thermal changes [30–32]. In this last case, this technique was also referred to as coda wave interferometry (CWI). Here CWI is applied to 1 kHz coda waves of the concrete dynamic response $h_\theta(t)$ to monitor the daily variations of temperature θ. Indeed, this impulse response does not only depend on the time t, but also on the temperature θ. In this experiment, nothing is supposed to change except temperature; in particular, the source and the receiver are supposed to be perfectly fixed.

The thermal change of the concrete structure results in a change in the wave velocities as follows:

$$c_P = c_P^0 + \Delta c_P, \quad c_S = c_S^0 + \Delta c_S, \tag{6}$$

where c^0 is the initial velocity at temperature θ_0, and Δc the shift due to rise in θ. For the sake of simplicity, we do not take into account thermal expansion of the concrete structure, which is one order of magnitude lower. At first order, it corresponds to a temporal dilation of the impulse response,

$$h_\theta(t) = h_{\theta_0}(t(1+\varepsilon)) \tag{7}$$

with ε the time dilation rate [31]. It is related to a delay δ in the coda around time t given by

$$\varepsilon = \frac{\delta}{t} \approx \frac{\Delta c}{c}. \tag{8}$$

This is a good approximation as long as the wave forms are weakly distorted. Distortion was carefully studied by Lobkis *et al.* [31] with ultrasounds in aluminum cavities. It is linked to different temperature dependence of c_P and c_S. In our concrete structure, it could also be due to changes in the diffraction patterns of the scatterers and is additionally subject to the spatial thermal variations in the structure. Distortion will be shortly discussed at the end Sec. III B.

B. Experimental setup

Like the first experiment presented in this paper, the experiment is conducted on the second floor of a concrete structure built with several coupled concrete slabs. An accelerometer (BK-4381) is placed 7 m away from a kHz seismic source (see Fig. 7). Strong attention was paid to the reproducibility of the source. In particular, a human hammer strike cannot remain perfectly reproducible over several hours. Thus, an electrically controlled vibration system (TIRA TV-51120) excited by a 10 s sweep $s(t)$ of frequencies linearly increasing from 20 Hz to 2000 Hz has been preferred. To reduce the noise, one response $r_\theta(t)$ of the concrete structure to the sweep at temperature θ results in the averaging of ten consecutive records. The 156 responses $r_\theta(t)$ have been recorded every 5 minutes during 13 hours, from midnight until 1:00 p.m. The signals $r_\theta(t)$ are then correlated with the sweep $s(t)$ to get an estimation of the impulse responses $h_\theta(t)$ of the structure (pulse compression)

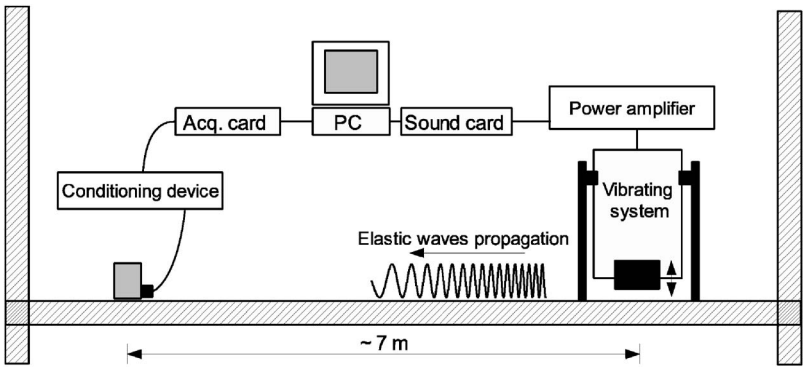

FIG. 7. Setup of the CWI experiment. A vibrating source (TIRA TV51120) sends a sweep in the concrete structure (frequency ranging from 20 Hz to 2000 Hz, sweep length = 10 s). The seismic acceleration is sensed 7 m away (BK-4381). Each sweep record is averaged ten times, defining one acquisition sequence. This sequence is repeated every 5 min from July 28th, 12:00 a.m. until July 28th, 1:00 p.m. The 5 min delay sets the temporal resolution of the monitoring.

$$h_\theta(t) = \int r_\theta(t+\tau)s(\tau)d\tau. \tag{9}$$

Wave forms recorded at 12:03 a.m. and 7:00 a.m. are displayed in Fig. 8. They correspond to a temperature decrease of $\Delta\theta \approx 3$ °C. The delay of direct waves (around $t=4$ ms) is not noticeable, but later in the coda, a clear delay is observed (0.18 ms in average around $t=40$ ms), which corresponds to a dilation rate $\varepsilon \approx 0.45\%$.

The delay δ between the two wave forms is defined following Lobkis *et al.* [31] and Snieder *et al.* [30] using the time-correlation $C^t_\theta(\tau)$:

$$C^t_\theta(\tau) = \frac{\int_{t+(t_W/2)}^{t-(t_W/2)} h_{\theta_0}(\nu)h_\theta(\nu+\tau)d\nu}{\sqrt{\int_{t+(t_W/2)}^{t-(t_W/2)} h^2_{\theta_0}(\nu)d\nu \int_{t+\frac{t_W}{2}}^{t-\frac{t_W}{2}} h^2_\theta(\nu)d\nu}}, \tag{10}$$

where θ and θ_0 are, respectively, the instantaneous and reference temperatures. The correlation is calculated for a time window t_W around the time t in the coda (which can be different and larger than the $\delta\tau$ of the CBE). The main features of the central peak composing this correlation are (1) the *delay* δ defined as the time τ of the maximum. Note that it should depend on the lapse time t in the coda and on temperature θ; (2) the *distortion*, which is quantified by $1-C^t_\theta(\delta)$, where $C^t_\theta(\delta)$ is the peak amplitude. It equals 0 for a perfect temporal dilation of the coda.

In Fig. 9, we present the measurement of the delay δ during 13 consecutive hours. Delays are calculated around the first arrivals ($t=4$ ms) and for multiply scattered and/or reflected waves ($t=40$ ms). The experiment was conducted in summertime (on July 28th) when very high thermal variations were observed outside. The outside temperature was indeed increasing from 17 °C (night) to 32 °C (1:00 p.m.). This resulted in noticeable variations of the concrete temperature: from 26 °C to 30 °C. From the structure's thermal variation (4 °C) and its delay estimation (=0.25 ms), we calculate that the thermal dilation rate of concrete velocities is 0.15%/°C [32]. At night, the structure was much warmer than outside and was slowly cooling down. During the daytime, the outside temperature is increasing very quickly and the structure is warming up. This is verified by the delay presented in Fig. 9, delay decreases at night and increases in

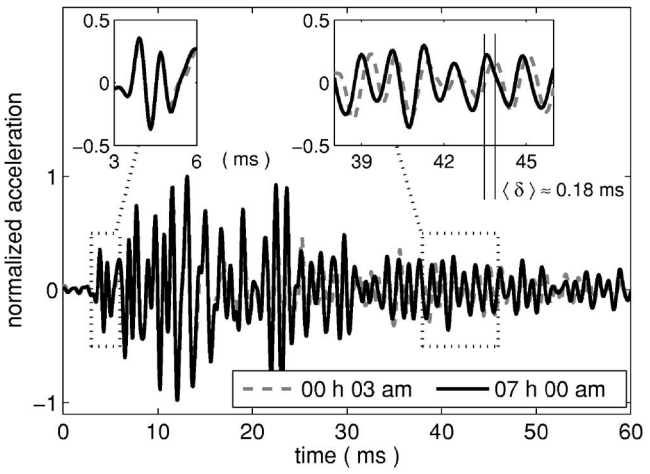

FIG. 8. Example of two dynamic responses at two different times: at midnight and at 7:00 a.m. The direct waves, i.e., the first ms of the records, do not change. Later in the coda, a slight delay d is observed. This delay is due to the weak thermal changes of the structure, resulting in an increase in the wave velocities. At night, the outside temperature is cold and the concrete structure is cooling down; therefore, the temperature at 12:03 a.m. is 3 °C lower than the one at 7:00 a.m. In this example, distortion, which changes the wave forms for varying temperature, is a very weak effect.

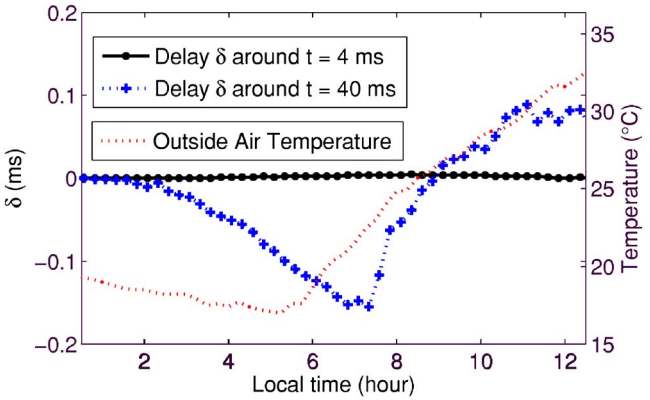

FIG. 9. (Color online) Delay d calculated around $t=4$ ms (direct waves) and around $t=40$ ms (multiply scattered and/or reverberated coda waves) for all the seismic impulse responses. The outside air temperature is displayed by a thin dotted line (not the temperature of concrete itself, which varies spatially). The velocity increases at night, resulting in a negative d. Starting from 7:00 a.m., the outside air and solar illumination are warming up the concrete structure. The velocity decreases which ultimately results in positive d.

the day. Due to the thickness of the slabs (20 cm) and thermal diffusion process, the variation of temperature inside the structure is both delayed ($\approx$1 h [32]) and attenuated compared to the outside temperature. In addition, spatial variations of temperature of the structure are noticeable: sometimes, variations of 4 °C within the structure were observed. Therefore, the delay δ is attributed to a thermal variation averaged over the structure, rather than the actual local change of temperature measured near the receiver.

From a practical point of view, our aim is to estimate the dilation ε with optimal precision. On the one hand, this requires going deep into the coda to measure a delay δ which varies linearly with time t [30–32]. On the other hand, distortion also increases with time t in the coda. Distortion was carefully studied in our experiment. From $t=0$ ms to $t=40$ ms, distortion is relatively negligible (ranging from 0% to 12%), allowing a good delay δ estimation. Later in the coda, distortion increases, and from $t=90$ ms on, temperature monitoring has become impossible. Distortion can have several origins. It is first due to different temperature dependences of c_P and c_S [31]. Second, it can be caused by changes in the diffraction patterns of scatterers and reverberations due to the dilatation. In our experiment, it is additionally due to the inhomogeneous thermal heating of the structure, which is clearly a strong limitation of our technique. The optimal lapse time is found to be $t=40$ ms in our experiment. Note that an in-depth study of distortion should give information on spatial variations of temperature and on the temperature dependencies of c_P and c_S.

IV. CONCLUSIONS

We have presented two different experiments aimed at studying the late arrivals (the coda) of the dynamic response of a concrete structure. These observations have revealed the presence of important information in the late part of the records, which might be relevant to engineering applications like nondestructive testing or concrete evaluation. They are performed in a complex structure made of several coupled 20-cm-thick concrete slabs of various dimensions and shapes. The seismic impulse response was acquired around 1 kHz using piezoelectric accelerometers glued on the principal slab. In the first experiment, the presence of multiple scattering or multiple diffractions in the coda was demonstrated using the coherent backscattering effect. This phenomenon allows a direct measurement of the scattering mean-free time without the bias of intrinsic absorption. We estimate it to be equal to $\approx$10 ms, implying the origin of coda waves to be multiple reverberations and diffractions, rather than internal scattering. At even higher frequencies [4,5], where diffuse waves are still present, this coherent backscattering technique would provide useful information on the concrete internal heterogeneity at a millimeter scale.

In the second experiment, we suggest coda wave interferometry (or diffuse wave spectroscopy) as one possible application of multiple diffraction, reverberations, and diffusion of waves around 1 kHz in concrete. This experiment was designed to monitor weak velocity changes in the structure due to strong outside thermal variations. To that aim we employed a perfectly reproducible seismic source and acquired the dynamic response of the structure every 5 min during 13 h. No variations were observed when looking at first arrivals (as do standard pulse-echo techniques). However, later in the diffuse part of the records, thermal variations resulted in a measurable dilation of the coda. Consequently, we obtain an estimate for the velocity change which would have been much more difficult to obtain with standard pulse-echo techniques. The precision obtained in this experiment is $\delta c/c=10^{-4}$. Because of important spatial variations, the internal temperature of the structure was very hard to evaluate; nevertheless, we estimated an average variation of $\sim$4 °C within 13 h, from which we deduced a thermal variation rate for velocities in concrete of 0.15%/°C. Now this dependence has been established, one could hope to correct for the thermal dilation of coda waves in order to monitor even weaker changes caused by other mechanisms. As it results in a similar coda dilation, we could, for instance, expect to quantify stress loading. Aging or cracking would have a different effect on coda waves and could be quantified by means of the distortion parameter. These are, of course, possible applications among others.

ACKNOWLEDGMENTS

The authors wish to thank R. L. Weaver, Ph. Roux, and A. Derode for fruitful discussions and advice, and Bruel&Kjaer for lending us the vibration system. The first author acknowledges a Lavoisier grant from the French Ministry of Foreign Affairs. We acknowledge the Laboratoire Central des Ponts et Chaussées (Nantes) for preliminary tests. This work was funded by the ACI "jeune chercheur" from the French Ministry of Research, and additionally supported by the GDR "ImCODE" of CNRS.

[1] O. Abraham, C. Lonard, P. Cte, and B. Piwakowski, ACI Mater. J. **97**, 645 (2000).
[2] M. Sansalone, J. M. Lin, and W. B. Streett, ACI Mater. J. **95**, 168 (1998).
[3] G. Hevin, O. Abraham, H. Pedersen, and M. Campillo, NDT & E Int. **31**, 289 (1998).
[4] S. K. Ramamoorthy, Y. Kane, and J. A. Turner, J. Acoust. Soc. Am. **115** (2), 523 (2004).
[5] P. Anugonda, J. S. Wiehn, and J. A. Turner, Ultrasonics **39**, 429 (2001).
[6] M. P. Van Albada and A. Lagendijk, Phys. Rev. Lett. **55**, 2692 (1985).
[7] P. E. Wolf and G. Maret, Phys. Rev. Lett. **55**, 2696 (1985).
[8] G. Maret and P. E. Wolf, Z. Phys. B: Condens. Matter **65**, 409 (1987).
[9] D. J. Pine, D. A. Weitz, P. M. Chaikin, and E. Herbolzheimer,

Phys. Rev. Lett. **60** (8), 1134 (1988).
[10] A. Derode, P. Roux, and Mathias Fink, Phys. Rev. Lett. **75**, 4206 (1995).
[11] A. Tourin, A. Derode, P. Roux, B. A. van Tiggelen, and M. Fink, Phys. Rev. Lett. **79**, 3637 (1997).
[12] A. Derode, E. Larose, M. Tanter, J. de Rosny, A. Tourin, M. Campillo, and Mathias Fink, J. Acoust. Soc. Am. **113**, 2973 (2003).
[13] A. Tourin, A. Derode, and M. Fink, Phys. Rev. Lett. **87**, 274301 (2001).
[14] O. I. Lobkis and R. L. Weaver, J. Acoust. Soc. Am. **110**, 3011 (2001).
[15] R. Hennino, N. Trégourès, N. M. Shapiro, L. Margerin, M. Campillo, B. A. van Tiggelen, and R. L. Weaver, Phys. Rev. Lett. **86**, 3447 (2001).
[16] E. Larose, L. Margerin, B. A. van Tiggelen, and M. Campillo, Phys. Rev. Lett. **93**, 48501 (2004).
[17] M. Campillo and A. Paul, Science **299**, 547 (2003).
[18] A. Kawabata, in *Anderson Localization*, edited by Y. Nagaoka *et al.* (Springer-Verlag, Berlin, 1982).
[19] G. Bayer and T. Niederdrank, Phys. Rev. Lett. **70**, 3884 (1993).
[20] G. Labeyrie, F. de Tomasi, JC Bernard, C. A. Muller, C. Miniatura, and R. Kaiser, Phys. Rev. Lett. **83**, 5266 (1999).
[21] B. A. van Tiggelen and R. Maynard, in *Wave Propagation in Complex Media*, edited by G. Papanicolaou (Springer, New York, 1998).
[22] J. de Rosny, A. Tourin, and M. Fink, Phys. Rev. Lett. **84**, 1693 (2000).
[23] L. Margerin, M. Campillo, and B. A. van Tiggelen, Geophys. J. Int. **145**, 593 (2001).
[24] D. Royer and E. Dieulesaint, *Elastic Waves in Solids, Part I. Free and Guided Propagation*, (Masson, Paris, 1996).
[25] G. Poupinet, W. L. Ellsworth, and J. Frechet, J. Geophys. Res. **89**, 5719 (1984).
[26] M. L. Cowan, I. P. Jones, J. H. Page, and D. A. Weitz, Phys. Rev. E **65**, 66605 (2002).
[27] M. L. Cowan, J. H. Page, and D. A. Weitz, Phys. Rev. Lett. **85**, 453 (2000).
[28] J. de Rosny and P. Roux, J. Acoust. Soc. Am. **109**, 2587 (2001).
[29] J. de Rosny, P. Roux, M. Fink, and J. H. Page, Phys. Rev. Lett. **90**, 94302 (2003).
[30] R. Snieder, A. Grët, H. Douma, and J. Scales, Science **295**, 2253 (2002).
[31] O. I. Lobkis and R. L. Weaver, Phys. Rev. Lett. **90**, 254302 (2003).
[32] D. Anache, M.S. dissertation, J. Fourier University, Grenoble, 2005 (Unpublished).